Inorg. Chem. **2006**, *45*, 1951–1959

Synthesis and Spectroscopic and Magnetic Characterization of Tris(3,5-dimethylpyrazol-1-yl)borate Iron Tricyanide Building Blocks, a Cluster, and a One-Dimensional Chain of Squares

Dongfeng Li,[†] Sean Parkin,[†] Guangbin Wang,[‡] Gordon T. Yee,[‡] and Stephen M. Holmes*,[†]

Department of Chemistry, University of Kentucky, Lexington, Kentucky 40506-0055, and Virginia Polytechnic Institute and State University, Blacksburg, Virginia 24061

Received June 24, 2005

The synthesis and spectroscopic and magnetic characterization of several hydridotris(3,5-dimethylpyrazol-1yl)-borate (Tp*) iron(II) and iron(III) tricyanide complexes, a rectangular cluster, and a one-dimensional chain of squares are described. Treatment of $[NEt_4][(Tp^*)Fe^{III}(CN)_3]$ (**3**) with manganese(II) triflate in dimethylformamide (DMF) affords rectangular clusters (**6**, $\{[(Tp^*)Fe(CN)_2(\mu\text{-}CN)Mn(DMF)_4]_2[OTf]_2\}\cdot 2DMF$), while tosylate salts afford one-dimensional networks (**5**, $\{Mn^{II}(DMF)_2(\mu\text{-}OTs)(\mu\text{-}NC)_2(NC)Fe^{III}(Tp^*)\}_n$) containing embedded $[(Tp^*)_2Fe^{III}{}_2Mn^{II}{}_2(CN)_6]^{2+}$ clusters via in situ trapping; the cluster and network crystallize in the monoclinic (**6**, $P2_1/n$) and triclinic (**5**, $P\bar{1}$) space groups, respectively. The 1-D network (**5**) appears to be derived from $\{cis\text{-}(\mu\text{-}O_3SC_6H_4Me)_2Mn^{II}(DMF)_4\}_n$ (**4**, $P2_1/n$), which is obtained via crystallization of $Mn(OTs)_2$ from DMF/Et_2O mixtures. For **4**, magnetic studies indicate that the Mn^{II} centers are magnetically isolated, with calculated J, g, and θ constants of 6.7×10^{-3} cm^{-1}, 2.03, and –0.52 K. Additional magnetic studies of **5** and **6** indicate that the $[(Tp^*)Fe^{III}(CN)_3]^-$ centers are highly anisotropic ($g = 2.9$) and are antiferromagnetically coupled to adjacent Mn^{II} centers. For **5** and **6**, fitting of the χT vs T data via the Curie–Weiss expression affords Curie (6.25 and 10.8 cm^3 K mol^{-1}) and Weiss (–14.37 and –8.80 K) constants that are consistent with antiferromagnetically coupled low-spin Fe^{III} and high-spin Mn^{II} centers; least-squares fitting of the χT vs T data using molecular field theory affords $g_{avg.}$, J_1, J_2, and J' values of 2.25, –1.72, –0.58, and –0.12 cm^{-1} for **5**. Overall, bridging tosylates appear to be poor communicators of spin information. For **6**, the g, J_1, and J_2 (2.15, –2.02, and –0.78 cm^{-1}) values were obtained via least-squares fitting of the χT vs T data using an expression derived using the Kambe vector coupling method; simulations of the data via MAGPACK afford $g_{avg.}$ and J_{iso} values of 2.1 and –2.1 cm^{-1}.

Introduction

Cyanometalates are a versatile class of inorganic building blocks that can be used to construct a variety of clusters and networks.[1–3] Cyanometalate complexes are excellent building blocks for rationally constructing molecule-based materials, because cyanides generally form linear μ-CN linkages between two metal centers, stabilize a variety of transition metal centers and oxidation states, and efficiently communicate spin density information.[1–3] The magnetic properties exhibited by these compounds can be described via pairwise exchange interactions that are mediated by the cyanide bridge with the sign of the local exchange interactions being predicted by simple molecular orbital symmetry analyses.[1–9]

* To whom correspondence should be addressed. E-mail: smholm2@uky.edu.
[†] University of Kentucky.
[‡] Virginia Polytechnic Institute and State University.

(1) Entley, W. R.; Girolami, G. S. *Science* **1995**, *268*, 397−400.
(2) Verdaguer, M.; Bleuzen, A.; Marvaud, V.; Vaissermann, J.; Seuleiman, M.; Desplanches, C.; Scuiller, A.; Train, C.; Garde, R.; Gelly, G.; Lomenech, C.; Rosenman, I.; Veillet, P.; Cartier, C.; Villain, F. *Coord. Chem. Rev.* **1999**, *190−192*, 1023−1047.
(3) Dunbar, K. R.; Heintz, R. A. *Prog. Inorg. Chem.* **1997**, *45*, 283−291.
(4) Holmes, S. M.; Girolami, G. S. *J. Am. Chem. Soc.* **1999**, *121*, 5593−5594.
(5) Hatlevik, Ø.; Buschmann, W. E.; Zhang, J.; Manson, J. L.; Miller, J. S. *Adv. Mater.* **1999**, *11*, 914−918.
(6) Dujardin, E.; Ferlay, S.; Phan, X.; Desplanches, C.; Cartier dit Moulin, C.; Sainctavit, P.; Baudelet, E.; Veillet, P.; Verdaguer, M. *J. Am. Chem. Soc.* **1998**, *120*, 11347−11352.
(7) Ferlay, S.; Mallah, T.; Ouahès, R.; Veillet, P.; Verdaguer, M. *Nature* **1995**, *378*, 701−703.
(8) Miller, J. S. *Chem. Eng. News* **1996**, *74* (3), 30−41.

10.1021/ic051044h CCC: $33.50
Published on Web 02/09/2006

However, to prepare robust molecular clusters with predictable and tunable properties, it is crucial to control the self-assembly of precursors during synthesis. Well-defined cyanometalate precursors or building blocks, that self-assemble with structures intact into a common structural archetype, are necessary for constructing materials that exhibit tunable properties.Through this "building-block approach", the magnetic, optical, and electronic properties of the resulting clusters can be altered in a systematic fashion, allowing for accurate magneto-structural correlations to be described.[1−9] A variety of bistable cyanometalates prepared via a building-block approach include single-molecule magnets (SMMs),[10−19] single-chain magnets (SCMs),[20−23] photomagnetic materials,[24−44] and room-temperature magnetic lattices.[4−7]

Of known cyanometalate clusters, the dominant structural building block contains $[fac\text{-}LM^n(CN)_3]^{n-3}$ (L = R_3tacn, triphos, Cp, Cp*) units where L is a facially coordinated tripodal ligand.[10,14−18,22,45−61] However, despite the prevalence of poly(pyrazolyl)borates in inorganic chemistry, surprisingly few of the cyanometalates have been reported. To date, only a single systematic effort to synthesize cyanometalate SMMs has been reported, and only recently has the role of spin−orbit coupling in these clusters been investigated.[12−19]

Recently, we and others have reported that facially capped tris- and tetra(pyrazolyl)borate tricyanide building blocks are useful synthons for constructing SMMs and SCMs.[14,19,23] The low-spin $[(Tp^{R,R})Fe^{III}(CN)_3]^-$ (R = H, Me; $S = {}^1/_2$) building blocks are magnetically anisotropic and exhibit significant orbital contributions to the magnetic moment ($g = 2.9$).[14,19,21,23] Only two tris(pyrazolyl)borate cyanometalate complexes were known prior to our studies, and many additional complexes can be synthesized via substitution of iron for other metal centers.[21,59]

As part of a continuing effort to prepare such materials, we have turned our attention toward molecular species that can be systematically substituted via a building-block ap-

(9) Gatteschi, D., Kahn, O., Miller, J. S., Palacio, F., Eds. *Magnetic Molecular Materials*; Kluwer: Dordrecht, The Netherlands, 1991.
(10) Sokol, J. J.; Hee, A. G.; Long, J. R. *J. Am. Chem. Soc.* **2002**, *124*, 7656−7657.
(11) Choi, H. J.; Sokol, J. J.; Long, J. R. *Inorg. Chem.* **2004**, *43*, 1606−1608.
(12) Berlinguette, C. P.; Vaughn, D.; Cañada-Vilalta, C.; Galán-Mascarós, J. R.; Dunbar, K. R. *Angew. Chem., Int. Ed.* **2003**, *42*, 1523−1526.
(13) Palii, A. V.; Ostrovsky, S. M.; Klokishner, S. I.; Tsukerblat, B. S.; Berlinguette, C. P.; Dunbar, K. R.; Galan-Mascaros, J. R. *J. Am. Chem. Soc.* **2004**, *126*, 16860−16867.
(14) Wang, S.; Zou, J.-L.; Zhou, H.-C.; Choi, H. J.; Ke, Y.; Long, J. R.; You, X.-Z. *Angew. Chem., Int. Ed.* **2004**, *43*, 5940−5943.
(15) Schelter, E. J.; Prosvirin, A. V.; Dunbar, K. R. *J. Am. Chem. Soc.* **2004**, *126*, 15004−15005.
(16) Dunbar, K. R.; Schelter, E. J.; Palii, A. V.; Ostrovsky, S. M.; Mirovitskii, V. Y.; Hudson, J. M.; Omary, M. A.; Klokishner, S. I.; Tsukerblat, B. S. *J. Phys. Chem. A* **2003**, *107*, 11102−11111.
(17) Schelter, E. J.; Prosvirin, A. V.; Reiff, W. M.; Dunbar, K. R. *Angew. Chem., Int. Ed.* **2004**, *43*, 4912−4915.
(18) Karadas, F.; Schelter, E. J.; Prosvirin, A. V.; Bacsa, J.; Dunbar, K. R. *Chem. Commun.* **2005**, 1414−1416.
(19) Li, D.; Parkin, S.; Wang, G.; Yee, G. T.; Prosvirin, A. V.; Holmes, S. M. *Inorg. Chem.* **2005**, *44*, 4903−4905.
(20) Lescouëzec, R.; Vaissermann, J.; Ruiz-Pérez, C.; Lloret, F.; Carrasco, R.; Julve, M.; Verdaguer, M.; Dromzee, Y.; Gatteschi, D.; Wernsdorfer, W. *Angew. Chem., Int. Ed.* **2003**, *42*, 1483−1486.
(21) Lescouëzec, R.; Vaissermann, J.; Lloret, F.; Julve, M.; Verdaguer, M. *Inorg. Chem.* **2002**, *41*, 818−826.
(22) Toma, L. M.; Lescouezec, R.; Lloret, F.; Vaissermann, J.; Verdaguer, M. *Chem. Commun.* **2003**, 1850−1851.
(23) Wang, S.; Zuo, J.-L.; Gao, S.; Song, Y.; Zhou, H.-C.; Zhang, Y.-Z.; You, X.-Z. *J. Am. Chem. Soc.* **2004**, *126*, 8900−8901.
(24) Sato, O. *Acc. Chem. Res.* **2003**, *36*, 692−700 and references therein.
(25) Arimoto, Y.; Ohkoshi, S.; Zhong, Z. J.; Seino, H.; Mizobe, Y.; Hashimoto, K. *J. Am. Chem. Soc.* **2003**, *125*, 9240−9241.
(26) Ohkoshi, S.; Hashimoto, K. *J. Am. Chem. Soc.* **1999**, *121*, 10591−10597.
(27) Sato, O.; Iyoda, T.; Fujishima, A.; Hashimoto, K. *Science* **1996**, *272*, 704−705.
(28) Sato, O.; Einaga, Y.; Iyoda, T.; Fujishima, A.; Hashimoto, K. *Inorg. Chem.* **1999**, *38*, 4405−4412.
(29) Shimamoto, N.; Ohkoshi, S.; Sato, O.; Hashimoto, K. *Inorg. Chem.* **2002**, *41*, 678−684.
(30) Bleuzen, A.; Lomenech, C.; Escax, V.; Villain, F.; Varret, F.; Cartier dit Moulin, C.; Verdaguer, M. *J. Am. Chem. Soc.* **2000**, *122*, 6648−6652.
(31) Cartier dit Moulin, C.; Villain, F.; Bleuzen, A.; Arrio, M.; Sainctavit, P.; Lomenech, C.; Escax, V.; Baudelet, F.; Dartyge, E.; Verdaguer, M. *J. Am. Chem. Soc.* **2000**, *122*, 6653−6658.
(32) Ohkoshi, S.-I.; Yorozu, S.; Sato, O.; Iyoda, T.; Fujishima, A.; Hashimoto, K. *Appl. Phys. Lett.* **1997**, *70*, 1040−1042.
(33) Ohkoshi, S.-I.; Einaga, Y.; Fujishima, A.; Hashimoto, K. *J. Electroanal. Chem.* **1999**, *473*, 245−249.
(34) Ohkoshi, S.-I.; Mizuno, M.; Hung, G.; Hashimoto, K. *J. Phys. Chem.* **2000**, *40*, 9365−9367.
(35) Mallah, T.; Thiebaut, M.; Verdaguer, M.; Veillet, P. *Science* **1993**, *262*, 1554−1557.
(36) Gu, Z.-Z.; Sato, O.; Iyoda, T.; Hashimoto, K.; Fujishima, A. *J. Phys. Chem.* **1996**, *100*, 18289−18291.
(37) Rombaut, G.; Golhen, S.; Ouahab, L.; Mathonière, C.; Kahn, O. *Dalton Trans.* **2000**, 3609−3614.
(38) Rombaut, G.; Golhen, S.; Ouahab, L.; Mathonière, C.; Kahn, O. *Inorg. Chem.* **2001**, *40*, 1151−1159.
(39) Ohkoshi, S.-I.; Machida, N.; Zhong, Z. J.; Hashimoto, K. *Synth. Met.* **2001**, *122*, 523−527.
(40) Rombaut, G.; Mathonière, C.; Guionneau, P.; Golhen, S.; Ouahab, L.; Verelst, M.; Lecante, P. *Inorg. Chim. Acta* **2001**, *326*, 27−36.
(41) Catala, L.; Mathonière, C.; Gloter, A.; Stephan, O.; Gacoin, T.; Boilot, J.-P.; Mallah, T. *Chem. Commun.* **2005**, 746−748.
(42) Herrera, J. M.; Marvaud, V.; Verdaguer, M.; Marrot, J.; Kalisz, M.; Mathonière, C. *Angew. Chem., Int. Ed.* **2004**, *43*, 5468−5471.
(43) Mathonière, C.; Podgajny, R.; Guionneau, P.; Labrugere, C.; Sieklucka, B. *Chem. Mater.* **2005**, *17*, 442−449.
(44) Dei, A. *Angew Chem., Int. Ed.* **2005**, *44*, 1160−1163.
(45) Shores, M. P.; Sokol, J. J.; Long, J. R. *J. Am. Chem. Soc.* **2002**, *124*, 2279−2292.
(46) Berseth, P. A.; Sokol, J. J.; Shores, M. P.; Heinrich, J. L.; Long, J. R. *J. Am. Chem. Soc.* **2000**, *122*, 9655−9662.
(47) Heinrich, J. L.; Sokol, J. J.; Hee, A. G.; Long, J. R. *J. Solid State Chem.* **2001**, *159*, 293−301.
(48) Sokol, J. J.; Shores, M. P.; Long, J. R. *Angew. Chem., Int. Ed.* **2001**, *40*, 236−239.
(49) Sokol, J. J.; Shores, M. P.; Long, J. R. *Inorg. Chem.* **2002**, *41*, 3052−3054.
(50) Yang, J. Y.; Shores, M. P.; Sokol, J. J.; Long, J. R. *Inorg. Chem.* **2003**, *42*, 1403−1419.
(51) Schelter, E. J.; Bera, J. K.; Basca, J.; Galán-Mascarós, J. R.; Dunbar, K. R. *Inorg. Chem.* **2003**, *42*, 4256−4258.
(52) Heinrich, J. L.; Berseth, P. A.; Long, J. R. *Chem. Commun.* **1998**, 1231−1232.
(53) Klausmeyer, K. K.; Wilson, S. R.; Rauchfuss, T. B. *J. Am. Chem. Soc.* **1999**, *121*, 2705−2711.
(54) Contakes, S. M.; Klausmeyer, K. K.; Milberg, R. M.; Wilson, S. R.; Rauchfuss, T. B. *Organometallics* **1998**, *17*, 3633−3635.
(55) Contakes, S. M.; Klausmeyer, K. K.; Rauchfuss, T. B. *Inorg. Chem.* **2000**, *39*, 2069−2075.
(56) Kuhlman, M. L.; Rauchfuss, T. B. *J. Am. Chem. Soc.* **2003**, *125*, 10084−10092.
(57) Contakes, S. M.; Kuhlman, M. L.; Ramesh, M.; Wilson, S. R.; Rauchfuss, T. B. *Proc. Natl. Acad. Sci.* **2002**, *99*, 4889−4893.
(58) Lescouëzec, R.; Vaissermann, J.; Lloret, F.; Julve, F.; Verdaguer, M. *Inorg. Chem.* **2002**, *41*, 5943−5945.
(59) Unpublished results. Withers, J. R.; Holmes, S. M. University of Kentucky, Lexington, KY, 2004.
(60) Kim, J.; Han, S.; Cho, I.-K.; Choi, K. Y.; Heu, M.; Yoon, S.; Suh, B. J. *Polyhedron* **2004**, *23*, 1333−1339.
(61) Wang, S.; Zuo, J.-L.; Zhou, H.-C.; Song, Y.; Gao, S.; You, X.-Z. *Eur. J. Inorg. Chem.* **2004**, *43*, 3681−3687.

proach, to afford compounds that exhibit tunable magnetic, electrical, and optical properties. Through these efforts, we hope to incorporate a series of aniosotropic centers to systematically prepare several SMM and SCM materials that exhibit high-spin ground states, large and negative axial zero-field splittings, and high blocking temperatures.[10−23,62−68] Herein, we report the preparation and characterization of a rectangular cluster and a cluster-expanded one-dimensional chain derived from tris(3,5-dimethylpyrazol-1-yl)borate iron(II,III) tricyanide building blocks.

Experimental Section

Materials. All operations were conducted under an argon atmosphere by using standard Schlenk and drybox techniques. Transfers of solutions containing cyanide were carried out through stainless steel cannulas. Solvents were distilled under dinitrogen from CaH_2 (acetonitrile), Mg turnings (methanol), or sodium-benzophenone (diethyl ether) and sparged with argon before use. Dimethylformamide (DMF) was dried using Linde 13X molecular sieves and sparged with argon prior to use. The preparation of Mn(OTs)$_2$,[69] Mn(OTf)$_2$,[70] and potassium hydridotris(3,5-dimethylpyrazol-1-yl)borate (KTp*)[71−74] are described elsewhere.

Physical Measurements. The IR spectra were recorded as Nujol mulls between KBr plates on a Mattson Galaxy 5200 FTIR instrument. UV−vis spectra were recorded under nitrogen using a Shimadzu UV-2501 PC UV−vis recording spectrophotometer. Magnetic measurements were conducted on a Johnson-Matthey magnetic susceptibility balance and a quantum design MPMS SQUID magnetometer. Diamagnetic corrections were estimated using Pascal's constants:[75−77] $\chi_{dia} = -325 \times 10^{-6}$ cm^3 mol^{-1} for **2**·H_2O, -322×10^{-6} cm^3 mol^{-1} for **3**·H_2O, 309×10^{-6} cm^3 mol^{-1} for **3**, -515×10^{-6} cm^3 mol^{-1} for **4**, -574×10^{-6} cm^3 mol^{-1} for **5**, and -922×10^{-6} cm^3 mol^{-1} for **6**. Microanalyses were performed by the University of Illinois Microanalysis Laboratory. Electrochemical measurements (cyclic voltammetry) were performed using a BAS CV-50W voltammetric analyzer. A three-electrode system was employed, consisting of a glassy carbon working electrode, a platinum wire counter electrode, and an Ag/AgCl reference electrode. Samples were measured with 0.1 mol L^{-1} [NBu$_4$]PF$_6$ as the supporting electrolyte, and ferrocene was added as an internal reference after each measurement. All potentials are reported relative to the ferrocene/ferrocenium (Cp_2Fe/Cp_2Fe^+, Fc/Fc^+) redox couple.

Synthesis of (Tp*)Fe(OAc) (1). (Tp*)Fe^{II}(OAc) was prepared using a modified procedure reported for (Tp*)Co^{II}(OAc) and (Tp*)Ni^{II}(OAc).[78] Dropwise addition of a 1:1 DMF/MeCN (40 mL) solution of KTp* (2.10 g, 6.25 mmol) into Fe(OAc)$_2$ (1.20 g, 6.90 mmol) in DMF (25 mL) over 30 min afforded a gray suspension. After 2 h, the mixture was evacuated to dryness at 50 °C; the gray residue was dissolved into MeCN (20 mL) and filtered, and Et_2O (30 mL) was added. The precipitated solid was isolated by filtration and was dried under vacuum (27 °C) for 2 h. Yield: 2.12 g (70%). IR (Nujol, cm^{-1}): 2517 (s), 1679 (vs), 1623 (vs), 1593 (vs), 1543 (vs), 1415 (vs), 1380 (vs), 1351 (vs), 1335 (vs), 1259 (s), 1200 (vs), 1089 (s), 1066 (vs), 1041 (vs), 1022 (s), 981 (s), 936 (m), 864 (m), 847 (s), 807 (vs), 773 (s), 698 (s), 664 (vs), 651 (vs), 617 (m), 462 (m). Note: Compound **1** is unstable in both solution and solid state under an argon atmosphere in the absence of light.

Synthesis of [NEt$_4$]$_2$[(Tp*)Fe(CN)$_3$]·H_2O (2·H_2O). Treatment of **1** in MeCN (20 mL) with [NEt$_4$]CN (2.92 g, 18.7 mmol) in MeCN (30 mL) afforded a reddish-brown solution that was allowed to stir for 4 h. The mixture was filtered to remove a brown, insoluble solid, and addition of Et_2O (90 mL) to the filtrate afforded an orange precipitate; recrystallization from MeCN/Et_2O mixtures afforded orange crystals of **2**·H_2O. Yield: 2.93 g (66.1%, KTp*-based). UV−vis (CH_3CN): λ_{max}/nm (ϵ_M/M^{-1} cm^{-1}) 424 (114), 363 (sh, 180), 325 (367). Anal. Calcd for $C_{34}H_{64}BN_{11}OFe$: C, 57.55; H, 9.09; N, 21.71. Found: C, 57.65; H, 9.24; N, 21.65. IR (Nujol, cm^{-1}): 3320 (s, br), 2507 (s), 2060 (vs), 2043 (vs), 1644 (m), 1544 (s), 1488 (vs), 1413 (vs), 1396 (vs), 1378 (vs), 1205 (vs), 1173 (vs), 1057 (s), 1001 (s), 814 (s), 785 (s), 722 (m), 693 (m), 647 (m). CV (CH_3CN, $c = 0.92 \times 10^{-3}$ M, scan rate = 100 mV s^{-1}): $E_c = -990$ mV ($i_c = 4.18$ μA), $E_a = -898$ mV ($i_a = 4.48$ μA), $E_{1/2} = -944$ mV. Anhydrous samples are obtained by drying crystals of **2**·H_2O under vacuum (27 °C) overnight. IR(Nujol/cm^{-1}): ν_{BH} 2501; ν_{CN} 2041 (s), 2017 (s).

Synthesis of [NEt$_4$][(Tp*)Fe(CN)$_3$]·H_2O (3·H_2O). Dropwise treatment of a 4:1 CH_2Cl_2/*i*-PrOH (50 mL) solution of **2** (2.00 g, 2.82 mmol) with aqueous 30% H_2O_2 (15 mL) rapidly afforded a red mixture. After 3 h, the aqueous phase was decanted and the organic layer was dried over anhydrous $MgSO_4$ and 4 Å molecular sieves. ***Caution:*** *Evacuating the mixture to dryness can cause detonation when magnetically stirred.* The red-brown solution was concentrated under vacuum (20 mL) and was layered with Et_2O (50 mL). The orange-red crystals that deposited after 3 days were isolated by filtration and dried in air overnight. Yield: 1.44 g (88.2%). Anal. Calcd for $C_{26}H_{46}N_{10}BO_2Fe$: C, 52.23; H, 7.78; N, 23.44. Found: C, 52.04; H, 8.01; N, 23.21. IR (Nujol, cm^{-1}): 3458 (s), 2528 (s), 2119 (s), 1628 (m), 1545 (vs), 1490 (s), 1416 (vs), 1394 (s), 1377 (vs), 1205 (s), 1184 (s), 1173 (s), 1061 (vs), 1001

(62) Barra, A.-L.; Caneschi, A.; Corina, A.; Fabrizi de Biani, F.; Gatteschi, D.; Sangregorio, C.; Sessoli, R.; Sorace, L. *J. Am. Chem. Soc.* **1999**, *121*, 5302−5310.
(63) Abbati, G. L.; Brunel, L.-C.; Casalta, H.; Corina, A.; Fabretti, A. C.; Gatteschi, D.; Hassan, A. K.; Jansen, A. G. M.; Maniero, A. L.; Pardi, L.; Paulsen, C.; Segre, U. *Chem. Eur. J.* **2001**, *7*, 1796−1807.
(64) Gatteschi, D.; Sorace, L. *J. Solid State Chem.* **2001**, *159*, 253−261.
(65) Collison, D.; Murrie, M.; Oganesyan, V. S.; Piligkos, S.; Poolton, N. R. J.; Rajaraman, G.; Smith, G. M.; Thomson, A. J.; Timco, G. A.; Wernsdorfer, W.; Winpenny, R. E. P.; McInnes, R. J. L. *Inorg. Chem.* **2003**, *42*, 5293−5303.
(66) Clérac, R.; Miyasaka, H.; Yamashita, M.; Coulon, C. *J. Am. Chem. Soc.* **2002**, *124*, 12837−12844.
(67) Gatteschi, D.; Sessoli, R. *Angew. Chem., Int. Ed.* **2003**, *42*, 268−297 and references therein.
(68) Caneschi, A.; Gatteschi, D.; Lalioti, N.; Sangregorio, C.; Sessoli, R.; Venturi, A.; Vindigni, A.; Rettori, A.; Pini, M. G.; Novak, M. A. *Angew. Chem., Int Ed.* **2001**, *40*, 1760−1763.
(69) Holmes, S. M.; McKinley, S. G.; Girolami, G. S.; Szalay, P. S.; Dunbar, K. R. *Inorg. Synth.* **2002**, *33*, 91−103.
(70) Holmes, S. M. Molecule-Based Magnets Constructed from Hexacyanometalates. Ph.D. Thesis, University of Illinois at Urbana-Champaign, Urbana, IL, 1999.
(71) Trofimenko, S.; Long, J. R.; Nappier, T.; Shore, S. G. *Inorg. Synth.* **1970**, *12*, 99−107.
(72) Trofimenko, S. *Scorpionates, The Coordination Chemistry of Polypyrazolylborate Ligands*; Imperial College Press: London, 1999; text and references therein.
(73) Trofimenko, S. *J. Am. Chem. Soc.* **1967**, *89*, 6288−6294.
(74) Trofimenko, S. *Chem. Rev.* **1993**, *93*, 943−980 and references therein.
(75) Carlin, R. L. *Magnetochemistry*; Springer-Verlag: New York, 1986.
(76) (a) Kahn, O. *Molecular Magnetism*; VCH Publishers: New York, 1993. (b) Goodenough, J. B. *Phys. Rev.* **1955**, *100*, 564−573. (c) Goodenough, J. B. *J. Phys. Chem. Solids* **1958**, *6*, 287−297. (d) Goodenough, J. B. *Magnetism and the Chemical Bond*; Interscience: New York, 1963. (e) Kanamori, J. *J. Phys. Chem. Solids* **1959**, *10*, 87−98.
(77) Wertz, J. E.; Bolton, J. R. *Electron Spin Resonance: Elementary Theory and Practical Applications*; Chapman and Hall: New York, 1986.
(78) Kikichi, S.; Sasakura, Y.; Yoshizawa, M.; Ohzu, Y.; Moro-oka, Y.; Akita, M. *Bull. Chem. Soc. Jpn.* **2002**, *75*, 1255−1262.

(s), 867 (m), 817 (m), 793 (s), 778 (s), 693 (m), 645 (m), 497 (m). μ_{eff} Found (μ_B): 2.53. Crystals of **3**·H_2O were dried under vacuum (27 °C) overnight to afford an orange powder; orange crystals (**3**) are obtained from dry MeCN/Et_2O mixtures after 24 h. UV−vis (CH_3CN): λ_{max}/nm (ϵ_M/M^{-1} cm^{-1}) 481 (sh, 130), 425 (267), 323 (87). Anal. Calcd for $C_{26}H_{42}N_{10}BFe$: C, 55.63; H, 7.54; N, 24.95. Found: C, 55.59; H, 7.48; N, 24.90. IR (Nujol, cm^{-1}): ν_{BH} 2549 (s); ν_{CN} 2115 (vs). CV (CH_3CN, $c = 3.53 \times 10^{-3}$ M, scan rate = 100 mV s^{-1}): $E_c = -998$ mV ($i_c = 18.6$ μA), $E_a = -890$ mV ($i_a = 19.7$ μA), $E_{1/2} = -944$ mV.

Synthesis of {$Mn^{II}(DMF)_2(\mu\text{-}OTs)_2$}$_n$ (4). A DMF (20 mL) solution of $Mn^{II}(OTs)_2$ (1.19 g, 3.0 mmol) was layered with Et_2O (40 mL) to afford colorless blocks after 2 days. The crystals were isolated by filtration, washed with Et_2O (10 mL), and dried under vacuum (27 °C) for 2 h. Yield: 1.63 g (100%). Anal. Calcd for $C_{20}H_{28}N_2O_8S_2Mn$: C, 44.16; H, 5.20; N, 5.15. Found: C, 44.66; H, 5.49; N, 4.87. IR (Nujol, cm^{-1}): 1655 (vs), 1391 (vs), 1378 (vs), 1234 (vs), 1175 (vs), 1131 (vs), 1114 (vs), 1049 (vs), 1016 (s), 819 (s), 683 (vs), 578 (s), 566 (s), 556 (s).

Synthesis of {$Mn^{II}(DMF)_2(\mu\text{-}OTs)(\mu\text{-}NC)_2(NC)Fe^{III}(Tp^*)$}$_n$ (5). Treatment of a DMF (15 mL) solution of **3** (0.500 g, 0.70 mmol) with $Mn(OTs)_2$ (0.800 g, 2.01 mmol) in DMF (15 mL) rapidly affords a red solution that was stirred for an additional 3 h. The red mixture was filtered, layered with Et_2O (50 mL), and allowed to stand 4 days. The red blocks were isolated by filtration, washed with Et_2O (10 mL), and dried under vacuum (27 °C) for 2 h. Yield: 0.20 g (35%). Anal. Calcd for $C_{31}H_{43}N_{11}BFeMnO_5S$: C, 46.30; H, 5.41; N, 19.17. Found: C, 45.90; H, 5.40; N, 18.90. IR (Nujol/KBr): 2527 (m), 2142 (vs), 2121 (m), 1660 (vs), 1542 (s), 1420 (vs), 1386 (vs), 1237 (vs), 1198 (vs), 1122 (s), 1061 (vs), 1045 (vs), 1014 (s), 819 (s), 682 (vs), 646 (m), 562 (s).

Synthesis of {$[(Tp^*)Fe(CN)_2(\mu\text{-}CN)Mn(DMF)_4]_2[OTf]_2$}·2DMF (6). Treatment of a DMF (15 mL) solution of **3** (0.400 g, 0.712 mmol) with $Mn(OTf)_2$ (0.780 g, 2.21 mmol) in DMF (15 mL) rapidly afforded a dark red mixture that was stirred for an additional 2 h. The red mixture was filtered, layered with Et_2O (50 mL), and allowed to stand 3 days. The dark red crystals were isolated by filtration, washed with Et_2O (10 mL), and dried under vacuum (27 °C) for 60 s. Yield: 0.580 g (81.4%). UV−vis (CH_3CN): λ_{max}/nm (ϵ_M/M^{-1} cm^{-1}) 541 (sh, 198), 456 (418). Anal. Calcd for $C_{62}H_{104}N_{26}B_2F_6O_{16}S_2Fe_2Mn_2$: C, 39.34; H, 5.55; N, 19.25. Found: C, 39.39; H, 5.51; N, 19.25. IR (Nujol, cm^{-1}): 2543 (m), 2158 (s), 2150 (s), 2119 (m), 1680 (s), 1651 (vs), 1543 (s), 1420 (s), 1378 (vs), 1274 (vs), 1263 (vs), 1223 (s), 1206 (s), 1151 (s), 1111 (s), 1062 (s), 1033 (s), 868 (m), 817 (m), 678 (s), 639 (vs), 518 (m). CV (CH_3CN, $c = 1.68 \times 10^{-3}$ M, scan rate = 100 mV s^{-1}): $E_c = -696$ mV ($i_c = 8.33$ μA), $E_a = -435$ mV ($i_a = 2.11$ μA).

Structure Determinations and Refinements. X-ray diffraction data were collected at 90.0(2) K on a Nonius kappaCCD diffractometer from irregular shaped crystals mounted in Paratone-N oil on glass fibers. Initial cell parameters were obtained (DENZO)[79] from ten 1° frames and were refined via a least-squares scheme using all data-collection frames (SCALEPACK).[79] Lorentz/polarization corrections were applied during data reduction. The structures were solved by direct methods (SHELXS97)[80] and completed by difference Fourier methods (SHELXL97).[80] Refinement was performed against F^2 by weighted full-matrix least-squares (SHELXL97),[80] and empirical absorption corrections (either SCALEPACK[79] or SADABS[81]) were applied. Hydrogen atoms were found in difference maps and subsequently placed at calculated positions using suitable riding models with isotropic displacement parameters derived from their carrier atoms. Non-hydrogen atoms were refined with anisotropic displacement parameters. Atomic scattering factors were taken from the *International Tables for Crystallography Vol. C*.[82] Crystal data, relevant details of the structure determinations, and selected geometrical parameters are provided in Tables 1, S1, and S2. Figures S2 and S3 were drawn using the CCDC Mercury (Version 1.3) program.

Results and Discussion

Synthesis and Spectroscopic Characterization. A variety of poly(pyrazolyl)borate tricyanide complexes have been prepared via ligand metathesis reactions. Treatment of iron(II) acetate with potassium tris(3,5-dimethylpyrazol-1-yl)borate (KTp*) in acetonitrile/dimethylformamide mixtures rapidly affords $(Tp^*)Fe^{II}(OAc)$ (**1**) in moderate yield. Compound **1** is extremely air-sensitive and is unstable in solution and solid form. Furthermore, **1** cannot be redissolved into acetonitrile, and freshly made, filtered solutions slowly precipitate an insoluble, cream-colored solid that exhibits an intense ν_{B-H} absorption at 2509 cm^{-1}; we presume (vide infra) that the solid is $(Tp^*)_2Fe^{II}$.[83] Attempts to obtain satisfactory elemental analyses of **1** consistently met with failure. The infrared spectrum of **1** (freshly precipitated) exhibits intense ν_{BH} (2517 cm^{-1}) and ν_{CO} (1679, 1623 cm^{-1}) stretching absorptions that are shifted to higher energies relative to those found for KTp* (2436 cm^{-1}) and $Fe(OAc)_2$ (1596 and 1539 cm^{-1}).[84]

Subsequent treatment of **1** with excess tetra(ethyl)ammonium cyanide in acetonitrile rapidly and cleanly affords a red hydrated iron(II) cyanometalate complex of $[NEt_4]_2$-$[(Tp^*)Fe^{II}(CN)_3]$·H_2O (**2**·H_2O) stoichiometry. The infrared spectrum of **2**·H_2O exhibits an intense ν_{BH} (2507 cm^{-1}) absorption that is shifted to lower energy relative to **1**, suggesting that greater electron density is present at the metal center; the ν_{CO} absorptions are also absent. Additional, intense absorptions that are assigned to lattice water (3320 cm^{-1}) and coordinated cyanides (2060, 2043 cm^{-1}) are readily apparent in the infrared spectrum.[84] The ν_{CN} stretching absorptions for **2**·H_2O are found at relatively low energies and are comparable to $K_4[Fe^{II}(CN)_6]$ (2044 cm^{-1}), Na[(tach)-$Fe^{II}(CN)_3$]·MeOH (tach = 1,3,5-triaminocyclohexane; 2052, 2014 cm^{-1}), and $[L_2Fe^{II}(CN)_2]$ (L = phen, 2079, 2065 cm^{-1}; L = bpy, 2070, 2078 cm^{-1}).[50,85−89] Anhydrous samples are also obtained by drying crystals of **2**·H_2O under vacuum,

(79) Otwinowski, Z.; Minor, W. *Methods Enzymol.* **1997**, *276*, 307−326.
(80) Sheldrick, G. M. *SHELX-97. Programs for Crystal Structure Solution and Refinement*; University of Gottingen: Gottingen, Germany, 1997.
(81) Sheldrick, G. M. *SADABS—An empirical absorption correction program*; Bruker Analytical X-ray Systems: Madison, WI, 1996.
(82) *International Tables for Crystallography Vol. C*; Kluwer Academic Publishers: Dordrecht, The Netherlands, 1992.
(83) Chanaka, D.; De Alwis, L.; Schultz, F. A. *Inorg. Chem.* **2003**, *42*, 3616−3622.
(84) Nakamoto, K. *Infrared and Raman Spectra of Inorganic and Coordination Compounds*, 5th ed., Part B; Wiley: New York, 1997; pp 54−58, 105−116.
(85) Watzky, M. A.; Endicott, J. F.; Song, X.; Lei, X.; Macatangay, A. *Inorg. Chem.* **1996**, *35*, 3463−3473.
(86) Zhan, S.; Meng, Q.; You, X.; Wang, G.; Zheng, P.-Z. *Polyhedron* **1996**, *15*, 2655−2658.
(87) Schilt, A. A. *Inorg. Synth.* **1970**, *12*, 247−251.
(88) Schilt, A. A. *J. Am. Chem. Soc.* **1960**, *82*, 3000−3005.

Table 1. Crystallographic Data for $[NEt_4]_2[(Tp^*)Fe(CN)_3]\cdot H_2O$ (**2·H₂O**), $[NEt_4][(Tp^*)Fe(CN)_3]\cdot H_2O$ (**3·H₂O**), $[NEt_4][(Tp^*)Fe(CN)_3]$ (**3**), $\{Mn(\mu\text{-}OTs)_2(DMF)_2\}_n$ (**4**), $\{Mn(DMF)_2(\mu\text{-}OTs)(\mu\text{-}NC)_2(NC)Fe(Tp^*)\}_n$ (**5**), and $[(Tp^*)Fe(CN)_3]_2[Mn(DMF)_4]_2[OTf]_2\cdot 2DMF$ (**6**)

	2·H₂O	**3·H₂O**	**3**	**4**	**5**	**6**
formula	$C_{34}H_{64}BN_{11}OFe$	$C_{26}H_{44}BN_{10}OFe$	$C_{26}H_{42}BN_{10}Fe$	$C_{20}H_{28}N_2O_8S_2Mn$	$C_{31}H_{43}BN_{11}O_5SFeMn$	$C_{68}H_{114}B_2F_6N_{28}O_{16}S_2Fe_2Mn_2$
formula wt	709.62	579.37	561.36	543.50	803.42	2001.19
crystal system	monoclinic	triclinic	trigonal	monoclinic	triclinic	monoclinic
space group	$P2_1/n$	$P\bar{1}$	$P3_1$	$P2_1/n$	$P\bar{1}$	$P2_1/n$
a, Å	18.3423(2)	9.5737(2)	9.7740(1)	14.8205(3)	10.5227(1)	15.295(3)
b, Å	11.6145(1)	10.0872(2)	9.7740(1)	5.2132(1)	11.8895(1)	13.194(3)
c, Å	18.9531(2)	17.4380(3)	26.1990(4)	16.2179(5)	15.8918(2)	24.321(5)
α, °	90	87.7452(6)	90	90	98.0687(5)	90
β, °	108.9596(5)	85.4244(7)	90	107.9202(12)	98.3582(5)	107.09(3)
γ, °	90	62.7646(8)	120	90	110.3618(5)	90
V, Å^3	3818.65(7)	1492.54(5)	2167.50(5)	1992.24(5)	1804.69(3)	4691.4(2)
D_c, g cm^{-3}	1.234	1.289	1.29	1.514	1.479	1.417
Z	4	2	3	2	2	2
μ, mm^{-1}	0.437	0.543	0.556	0.777	0.866	0.696
R_1[a]	0.0455	0.0367	0.0323	0.0348	0.0390	0.0655
wR_2[a]	0.0976	0.0797	0.0675	0.0874	0.0854	0.1801

[a] $I > 2\sigma(I)$, $R = \sum||F_o| - |F_o||\ \sum|F_o|$. $R_w = [(\sum w(|F_o| - |F_c|)^2/\sum wF_o^2)]^{1/2}$.

and the infrared spectrum exhibits ν_{BH} and ν_{CN} absorptions at 2501 and 2041 cm^{-1}, respectively.

Oxidation of **2·H₂O** with aqueous hydrogen peroxide readily affords a new iron(III) tricyanide complex of $[NEt_4][(Tp^*)Fe^{III}(CN)_3]\cdot H_2O$ (**3·H₂O**) stoichiometry. Cyclic voltamograms of **2·H₂O** and **3** in acetonitrile exhibit reversible waves at $E_{1/2} = -944$ mV vs. Fc^+/Fc as expected. The $[(Tp^*)Fe(CN)_3]^{2-/-}$ redox couple is much lower than $[(Me_3tacn)Fe(CN)_3]^{0/-}$ (MeCN, −640 mV vs. Fc/Fc^+) and close to that found for $[Fe(CN)_6]^{4-/3-}$ (−921 mV in MeCN vs. Fc/Fc^+), suggesting that **2·H₂O** and **3** are electron-rich complexes.[90] The infrared spectrum of **3·H₂O** exhibits cyano- and borohydride stretching absorptions at 2119 and 2528 cm^{-1}, repectively, that are shifted to higher energies relative to **2·H₂O**, suggesting that oxidation of the iron center decreased charge delocalization via π back-bonding is present; a ν_{OH} stretching absorption attributed to lattice water is also found at 3458 cm^{-1}.[84] Anhydrous samples (**3**) exhibit significantly higher energy ν_{BH} and slightly lower energy ν_{CN} absorptions at 2549 and 2115 cm^{-1}, respectively. The cyano stretching absorption exhibited by **3·H₂O** is comparable to those seen for $K_3Fe^{III}(CN)_6$ (2135 cm^{-1}) and $[PPh_4][LFe^{III}(CN)_4]$ (L = phen, 2120 cm^{-1}; L = bpy, 2118 cm^{-1}); the structurally related complexes, $[(tach)Fe^{III}(CN)_3]\cdot H_2O$ and $[cat][(Tp)Fe^{III}(CN)_3]\cdot 2H_2O$ (cat = PPh_4^+, K^+), exhibit ν_{CN} absorptions at 2121 and 2123 cm^{-1}, respectively.[85,91−94] While the ν_{BH} absorption energy has not been reported for the tris(pyrazolyl)borate complexes, we find that $[PPN][(Tp)Fe^{III}(CN)_3]$ exhibits ν_{BH} and ν_{CN} absorptions at 2527 and 2117 cm^{-1}, respectively.[59,84]

Treatment of **3** with anhydrous manganese(II) *p*-toluenesulfonate in DMF affords red crystals of $\{Mn^{II}(DMF)_2(\mu\text{-}OTs)(\mu\text{-}NC)_2(NC)Fe^{III}(Tp^*)\}_n$ (**5**) stoichiometry. The infrared spectrum of **5** exhibits intense ν_{BH} (2527 cm^{-1}) and ν_{CN} (2142 cm^{-1}) stretching absorptions that are shifted to higher energies relative to **3** and **3·H₂O**, suggesting the formation of $Fe^{III}-CN-Mn^{II}$ linkages, and are comparable to clusters of $[(Tp)Fe^{III}(CN)_3]_2[Mn^{II}(MeOH)_4]\cdot 2MeOH$ (2128, 2151 cm^{-1}) and $\{[(Tp)Fe^{III}(CN)_3]_{2-}[Mn^{II}(bpy)_2]_2[ClO_4]_2\}\cdot 4MeCN$ (2148 cm^{-1}) stoichiometry.[60,61] The high-energy ν_{CN} absorption is consistent with the formation of $Fe^{III}-CN-Mn^{II}$ units and depopulation of the cyanide 5σ orbital.[84] Additional ν_{CN} and ν_{CO} stretching absorptions, found at 2121 and 1660 cm^{-1}, respectively, are tentatively assigned to terminal cyanides and coordinated DMF.

However, upon treatment of **3** with manganese(II) trifluoromethanesulfonate in DMF, a tetranuclear rectangular cluster of $\{[(Tp^*)Fe^{III}(CN)_3M^{II}(DMF)_4]_2[OTf]_2\}\cdot 2DMF$ (**6**) stoichiometry is obtained. The infrared spectrum exhibits several ν_{CN} stretching absorptions at 2158, 2150, and 2119 cm^{-1}, in addition to an intense ν_{BH} absorption at 2543 cm^{-1}. Two of the cyanide stretching absorptions are shifted to higher energies, relative to **3** and **3·H₂O**, and are probably due to bridging cyanides.[60,61] For **6**, an additional ν_{CN} absorption (2121 cm^{-1}) is present, being close in energy to those observed for **3** and **3·H₂O**. We propose that both bridging and terminal cyanides are present in **6**.

Crystallographic Studies. The tricyanometalate complexes are C_{3v} symmetric, six-coordinate $[fac\text{-}(Tp)Fe^n(CN)_3]^{(n-4)}$ salts that crystallize in the monoclinic ($P2_1/n$, **2·H₂O**), trigonal ($P3_1$, **3**), and triclinic ($P\bar{1}$, **3·H₂O**) space groups, respectively (Table 1, Figures 1and S2 and S4 in Supporting Information). The Fe−C bond distances range from 1.899(2) to 1.908(2) Å for **2·H₂O**, 1.917(3) to 1.930(3) Å for **3**, and 1.929(2) to 1.935(2) Å for **3·H₂O** (Table S1 in Supporting Information). The smallest Fe−C bond distances are found for **2·H₂O**, while comparatively longer values are exhibited by the Fe^{III} derivatives (**3** and **3·H₂O**). If the Fe−C bond distances are scaled as a function of iron oxidation state, the shortest bond distances should be found

(89) Nieuwenhuyzen, M.; Bertram, B.; Gallagher, J. F.; Vos, J. G. *Acta Crystallogr., Sect. C* **1998**, *54*, 603−606.
(90) Moreland, A. C.; Rauchfuss T. B. *Inorg. Chem.* **2000**, *39*, 3029−3036.
(91) Lescouëzec, R.; Lloret, F.; Julve, M.; Vaissermann, J.; Verdaguer, M.; Llusar, R.; Uriel, S. *Inorg. Chem.* **2001**, *40*, 2065−2072.
(92) Lescouëzec, R.; Lloret, F.; Julve, M.; Vaissermann, J.; Verdaguer, M. *Inorg. Chem.* **2002**, *41*, 818−826.
(93) Oshio, H.; Tamada, O.; Onodera, H.; Ito, T.; Ikoma, T.; Tero-Kubota, S. *Inorg. Chem.* **1999**, *38*, 5686−5689.
(94) Chakov, N. E.; Wernsdorfer, W.; Abboud, K. A.; Christou, G. *Inorg. Chem.* **2004**, *43*, 5919−5930.

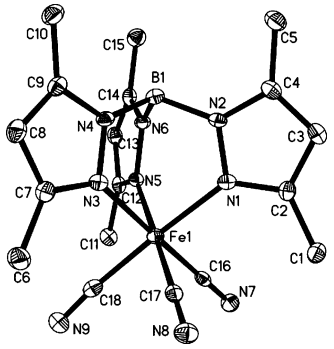

Figure 1. Truncated X-ray structure of **2·H₂O**. Thermal ellipsoids are at the 50% level, and all cations, hydrogen atoms, and lattice waters are removed for clarity.

for the trivalent complexes **3** and **3**·H_2O. However, the opposite trend is observed, suggesting that Fe^{II} derivatives exhibit enhanced π back-bonding relative to trivalent analogues.[50,85−94]

The Fe−N bond distances and C−Fe−C bond angles only slightly vary for the tricyanometalate anions. The average Fe−N bond distances range from 2.004(3) to 2.053(2) Å, while the C−Fe−C bond angles range from 86.73(8) to 90.39(8)° for **2**·H_2O, 85.8(1) to 92.0(1)° for **3**, and 84.55(7) to 91.34(7)° for **3**·H_2O; the average N−Fe−N bond angles are 87.57(7), 89.36(9), and 89.03(6)°, for **2**·H_2O, **3**, and **3**·H_2O, respectively (Tables S1 and S2 in Supporting Information). Relative to [cat][(Tp)$Fe^{III}$$(CN)_3$]·$2H_2O$ (cat = PPh_4^+, PPN^+), **3** and **3**·H_2O probably exhibit longer Fe−C and Fe−N bonds and smaller C−Fe−C bond angles, due to greater electron donation and steric demand of the Tp* ligand relative to Tp.[58,71−74]

Crystals of **2**·H_2O also contain lattice water that is hydrogen-bonded to cyanide nitrogen atoms (N(7) and N(8)) forming anionic one-dimensional helical chains along the crystallographic *a* direction; the O(1W)···N(7) and O(1W)···N(8) contacts are 2.872(2) and 2.853(2) Å, respectively (Table S1 and Figure S1 in Supporting Information).[102] Likewise, compound **3**·H_2O exhibits one-dimensional hydrogen bonding between cyanide (N_7 and N_8) and lattice water that propagates along the crystallographic *c* direction (zigzag chain); the O(1W)···N(7) and O(1W)···N(8) contacts are 3.012(2) and 2.998(2) Å (Table S1 and Figure S3 in Supporting Information).[102]

Compound **4** crystallizes in the monoclinic ($P2_1/n$) space group and adopts a one-dimensional chain motif containing embedded {*trans*-$Mn(DMF)_2(\mu\text{-}OTs)_2\}_n$ rectangles (Figures 2 and S5 in Supporting Information). The mutually cis

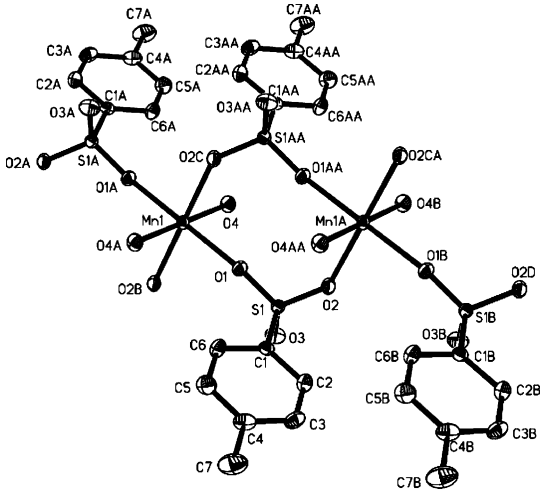

Figure 2. Fragment of the one-dimensional chain present in **4** along the crystallographic *a* direction. Thermal ellipsoids are at the 50% level, hydrogen atoms are removed, DMF ligands are truncated, and only oxygen, carbon, manganese, and sulfur atoms are illustrated for clarity.

bridging tosylates link adjacent D_{4h}-symmetric Mn^{II} centers (equatorial sites), while two DMF ligands are found in the axial positions. The structure of **4** can be considered as an alternating array of cationic Mn^{II} centers linked to adjacent *trans*-$[Mn^{II}(OH_2)_2(\mu\text{-}OTs)_4]^{2-}$ units via tosylate oxygen atoms and is structurally similar to a cadmium network reported by Loiseleur of $\{Cd(OH_2)_2(O_3SC_6H_4Me)_2\}_\infty$ stoichiometry.[95]

For **4**, each *p*-tolyl ring is parallel to the coordinated DMF ligands and terminal sulfoxide functionalities. The S(1)−O(1), S(1)−O(2), and Mn(1)−O(1) bond distances are 1.452(2), 1.468(2), and 2.159(2) Å, while the O(1)−S(1)−O(2), O(1)−Mn(1)−O(2B), and O(1)−Mn(1)−O(2B) bond angles are 112.00(9), 88.35(5), and 88.35(5)°. The O−S−O and O−Mn−O bond angles indicate that the sulfur and manganese centers adopt distorted tetrahedral and octahedral geometries, respectively (Tables S1 and S2). The Mn(1)···Mn(1A) and S(1)···S(1B) contacts are 5.213(3) and 4.566(3) Å, respectively (Figure S5 and Table S1).[18]

Compound **5** crystallizes in the triclinic ($P\bar{1}$) space group and is structurally related to **4**. The one-dimensional network consists of cationic $\{cis\text{-}Mn^{II}(\mu\text{-}OTs)_2Mn^{II}\}^{2+}$ squares that are linked via cyanides to two adjacent $[(Tp^*)Fe^{III}(CN)_3]^-$ units; two trans DMF ligands complete the coordination sphere of each Mn^{II} center (Figures 3 and S6 in Supporting Information). Alternatively, **5** can be considered to be a structural analogue of **4**, via substitution of alternate tosylate anions for $[(Tp^*)Fe(CN)_3]^-$. Nevertheless, **5** is a neutral one-dimensional chain of $\{Mn(DMF)_2(\mu\text{-}OTs)(\mu\text{-}NC)_2(NC)Fe(Tp^*)\}_n$ stoichiometry.

In **5**, the coordinated DMF and tosylate tolyl rings are parallel and roughly perpendicular to the terminal sulfoxide functionalities of the bridging tosylates. The S(1)−O(1), Mn(1)−O(1), Mn(1)−N(7), and Fe(1)−C(16) bond distances are 1.457(2), 2.166(2), 2.233(2), and 1.918(2) Å, respectively, while the O(1)−S(1)−O(3), O(1)−Mn(1)−O(1A), N(7)−Mn(1)−O(1), and C(16)−Fe(1)−C(17) bond angles are 112.4(1), 91.28(6), 177.37(7), and 86.37(9)°, respectively

(95) Charbonnier, F.; Faure, R.; Loiseleur, H. *Acta Crystallogr., Sect. B* **1978**, *34*, 1504−1506.
(96) Borrás-Alemar, J. J.; Burriel, R.; Coronado, E.; Gatteschi, D.; Gómez-Garcia, C. J.; Zanchini, C. *Inorg. Chem.* **1991**, *30*, 947−950.
(97) Lescouëzec, R.; Lloret, F.; Julve, M.; Vaissermann, J.; Verdaguer, M. *Inorg. Chem.* **2002**, *41*, 818−826.
(98) Borras-Almenar, J. J.; Clemente-Juan, J. M.; Coronado, E.; Tsukerblat, B. S. *J. Comput. Chem.* **2001**, *22*, 985−991.
(99) Borras-Almenar, J. J.; Clemente-Juan, J. M.; Coronado, E.; Tsukerblat, B. S. *Inorg. Chem.* **1999**, *38*, 6081−6088.
(100) Kambe, K. *J. Phys. Soc. Jpn.* **1950**, *5*, 48−51.
(101) Myers, B. E.; Berger, L.; Friedberg, S. A. *J. Appl. Phys.* **1969**, *40*, 1149−1151.
(102) See the Supporting Information.

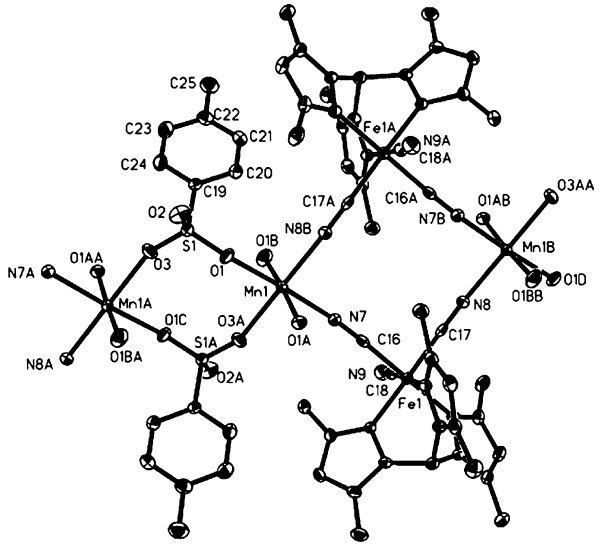

Figure 3. Fragment of the one-dimensional chain present in **5** along the crystallographic *a* direction. Thermal ellipsoids are at the 50% level, hydrogen atoms are eliminated, and only DMF oxygen atoms are illustrated for clarity.

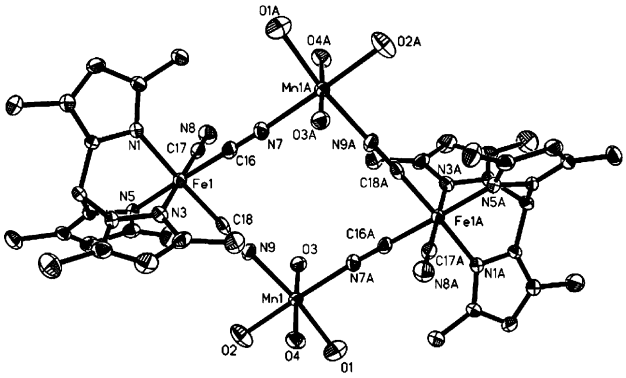

Figure 4. Truncated X-ray structure of **6**. Thermal ellipsoids are at the 50% level, and all anions, hydrogen atoms, and lattice DMF are eliminated. Only coordinated DMF oxygen atoms are illustrated for clarity.

(Tables S1 and S2). The Mn(1)···Mn(1A) (5.476(3) Å) and S(1)···S(1A) (4.631(3) Å) interactions are longer than those of **4**, while the Mn(1)···Mn(1B) and Fe(1)···Fe(1A) interactions are 7.390(3) and 7.435(3) Å, respectively (Table S1)[18]

Compound **6** is a cationic tetranuclear cluster that crystallizes in the monoclinic $P2_1/n$ space group.[19] The Fe^{III} and Mn^{II} centers reside in alternate corners of the rectangular cluster and are also linked via cyanides (Figure 4). A third terminal cyanide per $[(Tp^*)Fe(CN)_3]^-$ center remains, and these are related by an inversion center, in an anti orientation relative to the Fe_2Mn_2 plane. A single methyl group per Tp* ligand projects perpendicular to and above (2.952(3) Å) the Fe_2Mn_2 plane, located opposite the terminal cyanides; structural analogues of **6** have also been reported by Dunbar, Verdaguer, Kim, Oshio, and co-workers.[18,21−22,60]

In comparison to **5**, the tetranuclear Fe_2Mn_2 cluster (**6**) is slightly compressed with respect to metal-cyanide and cluster edge lengths. The Fe(1)−C(16), Fe(1)−C(17), Fe(1)−C(18), Mn(1)−N(9), and Mn(1)−N(7A) bond distances are 1.914(5), 1.938(6), 1.916(5), 2.178(4), and 2.195(4), respectively, while the C(16)−Fe(1)−C(17), C(16)−Fe(1)−C(18), and N(7A)−Mn(1)−N(9) bond angles are 86.8(2), 85.0(2), and 93.82(2)°, respectively; the closest Tp* ring contacts are 3.649(3) Å (Tables S1 and S2). The Fe−C and Mn−N bond distances for **6** are virtually identical to **5**, while the diagonal Mn(1)···Mn(1A) (7.108(3) Å) and Fe(1)···Fe(1A) (7.733(3) Å) contacts are ca. 0.28 Å smaller (Table S1).[19]

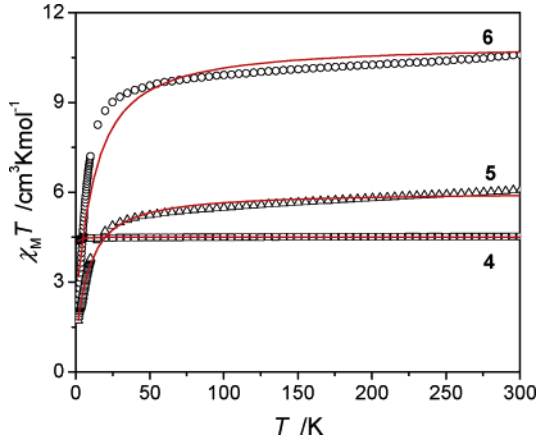

Figure 5. Temperature dependence of χT for **4** (□), **5** (△), and **6** (○) in an applied dc field of 1 kG. The red lines represent the best fit of the data (see text for details).

Magnetic Studies. The temperature dependence of $\chi_M T$ suggests that the Mn^{II} centers in **4** are magnetically isolated between 300 and 1.8 K. As judged from the χT vs T data using crushed crystals, the χT product decreases slightly, from 4.52 to 4.38 cm^3 K mol^{-1}, as the temperature is lowered from 300 to 1.8 K (Figure 5). The $\chi_M T$ values over this temperature range are close to those expected (4.375 cm^3 K mol^{-1}) for a noninteracting array of isotropic Mn^{II} centers. Fitting of the magnetic susceptibility data to the Curie−Weiss expression affords Curie and Weiss constants of 4.52 cm^3 K mol^{-1} and −0.52 K, respectively.

Further analysis of the temperature dependence of χT verifies that the Mn^{II} centers are magnetically isolated. This is done by using a modified expression for a classical Heisenberg chain (eq 1)

$$\chi_M = \frac{2Ng^2\beta^2S(S+1)}{3kT}\frac{1-u}{1+u} \qquad (1)$$

where $u = -\coth K + 1$, $K = JS(S+1)/kT$, $S = {}^5/_2$, and the exchange Hamiltonian is $H = -JS_1S_2$; values of J and g are calculated to be 6.7×10^{-3} cm^{-1} and 2.03, respectively.[96] Furthermore, ac susceptibility measurements suggest that χ'' is frequency-independent and does not exhibit the ferromagnetic maximum because of spin canting, reported for Mn^{II}_2(EDTA)·H_2O.[96,102] Consequently, we conclude that **4** is a paramagnetic solid and tosylate-mediated superexchange is inefficient above 2 K.

For **5** and **6**, the carbon-bound cyanides in each rectangular Fe_2Mn_2 fragment give rise to low-spin Fe^{III} ($S = {}^1/_2$) centers, which are expected to exhibit orbital contributions to the magnetic moment.[14,19,51,60,61] Consequently, spin-only formulas are not expected to be relevant. Using the temperature dependence of the χT product for **4** as a reference point, the magnetic anisotropy of the low-spin Fe^{III} centers present in **5** and **6** can be approximated. Assuming that the Mn^{II} centers

in **5** and **6** are also high-spin and that g_{Mn} is 2, a g_{Fe} value of ca. 2.9 can be calculated from the χT data (crushed crystals).

Subsequent measurements using crushed crystals of **3**·H_2O confirm that g (2.92) deviates significantly from 2 (Figure S7 in Supporting Information). The χT value monotonically decreases from 0.74 cm^3 K mol^{-1} to 0.56 cm^3 K mol^{-1} as the temperature is lowered from 300 to 1.8 K. The room-temperature value of χT is significantly larger than the spin-only value expected for isolated low-spin iron(III) centers (0.375 cm^3 K mol^{-1} for $S = {}^1/_2$, assuming $g = 2$). The observed decrease in χT as a function of decreasing T is attributable to depopulation of the thermally populated states that are spin−orbit coupled to the $^2T_{2g}$ ground state.[97]

The temperature dependence of χT for **6** suggests that the Fe^{III} and Mn^{II} centers couple antiferromagnetically (Figure 5). Between 300 and 35 K, the χT values gradually decrease from 10.60 to 9.63 cm^3 K mol^{-1} and then more abruptly decrease below ca. 10 K, reaching a minimum value of 1.99 cm^3 K mol^{-1} at 1.8 K; similar behavior has been reported by Kim et al.[60] and Wang et al.[61] for clusters of $[(Tp)Fe(CN)_3]_2[Mn(MeOH)_4]$ and $[(Tp)Fe(CN)_3]_2[Mn(bpy)_4]_2[ClO_4]_2$ stoichiometry.[60,61] Furthermore, ac susceptibility measurements indicate that χ'' is frequency-independent, suggesting that **6** is not a single-molecule magnet.[102] We propose that zero-field splitting of the $S = 4$ ground state at low temperatures affords lower-than-expected χT values rather than intercluster antiferromagnetic interactions, since the closest pyrazole-ring contacts between clusters are 5.434(4) Å.[19,96]

Goodenough and Kanamori describe that superexchange between low-spin Fe^{III} and Mn^{II} centers should be antiferromagnetic due to spin state and orbital symmetry considerations.[76] Assuming for simplicity, that the Mn^{II} ($t_{2g}^3e_g^2$) centers are octahedral, the low-spin Fe^{III} (t_{2g}^5) centers should engage in antiferromagnetic exchange with each adjacent Mn^{II} ion.[75] Nonlinear least-squares fitting of the magnetic data via the Curie−Weiss equation verifies that these simple, simplified orbital symmetry arguments are applicable, as antiferromagnetic coupling is observed between the cyanide-bridged Fe^{III} and Mn^{II} centers. The sign and relative magnitudes of θ in **5** and **6** (−14.37 and −8.80 K) are comparable to those for the hexacyanoferrate(III) network of $\{Mn(OH_2)_2[Mn(bpym)(OH_2)]_2[Fe(CN)_6]_2\}_\infty$ ($\theta = -12.8$ K) stoichiometry; the corresponding Curie constants are 6.25 and 10.8 cm^3 K mol^{-1} for **5** and **6**, respectively. Simulations of the χT vs T data using MAGPACK[98,99] allowed for estimations of $g(M^{II})$ and J_{iso}, affording values of 2.1 and −2.1 cm^{-1} for **6**.[19,102]

The dc susceptibility data for **6** was also modeled as a four-spin system that exhibits three exchange coupling constants representing the magnetic interactions between adjacent Fe^{III}−Mn^{II} (J_1) and diagonal $Fe^{III}\cdots Fe^{III}$ (J_2) and $Mn^{II}\cdots Mn^{II}$ (J_3) units. Using an isotropic Heisenberg Hamiltonian, the following relationship is obtained (eq 3):

$$\hat{H} = -2J_1(\hat{S}_1\cdot\hat{S}_2 + \hat{S}_2\cdot\hat{S}_3 + \hat{S}_3\cdot\hat{S}_4 + \hat{S}_4\cdot\hat{S}_1) - 2J_2(\hat{S}_2\cdot\hat{S}_4) - 2J_3(\hat{S}_1\cdot\hat{S}_3) \quad (2)$$

Further simplification of eq 2, assuming that $J_2 \approx J_3$, yields a simplified Hamiltonian of the following form:

$$\hat{H} = -2J_1(\hat{S}_1\cdot\hat{S}_2 + \hat{S}_2\cdot\hat{S}_3 + \hat{S}_3\cdot\hat{S}_4 + \hat{S}_4\cdot\hat{S}_1) - 2J_2(\hat{S}_2\cdot\hat{S}_4 + \hat{S}_1\cdot\hat{S}_3) \quad (3)$$

An expression for $\chi_M T$ was derived using the Kambe vector coupling method, and the dc susceptibility data was fitted via eq 4.[93,100,102] The values of $g_{avg.}$, J_1, and J_2 for **6** were obtained via least-squares fitting of the $\chi_M T$ versus T data and are found to be 2.15, −2.02, and −0.78 cm^{-1}, respectively.[102]

If superexchange interactions through the bridging tosylates are neglected for **5**, the one-dimensional chain of squares can be treated as an array of noninteracting and magnetically isolated $Fe^{III}_2Mn^{II}_2$ clusters. Least-squares fitting of the $\chi_M T$ data afford g_{iso}, J_1, and J_2 values of 2.62, −2.03, and −0.72 cm^{-1}, respectively.[102] However, if nonzero cluster−cluster exchange interactions (J') are present, then the temperature dependence of the magnetic susceptibility can be described using molecular field theory, via eq 4,

$$\chi_M = \frac{\chi}{1 - 4zJ'\chi/Ng^2\beta^2} \quad (4)$$

where z is the number of interacting clusters.[101] For $z = 2$, with least-squares fitting of the χ_M vs T data (eq 4), we obtain g, J_1, J_2, and J' values of 2.25, −1.72, −0.58, and −0.12 cm^{-1}, respectively.[102] The cluster-expanded chains (**5**) appear to exhibit slightly greater anisotropy and smaller exchange couplings between adjacent manganese(II) and iron(III) centers, relative to **6**; ac susceptibility measurements also indicate that χ'' is frequency-independent. The calculations suggest that **5** is a one-dimensional chain of weakly interacting magnetic squares.

The field dependence of the magnetization for **5** and **6** suggests that nonlinear magnetization vs. applied field effects that grow faster than the Brillouin functions are operative.[66−68,75,76,102] At 1.8 K, the magnetization values are 3.3 and 6.8 μ_B, suggesting $S = 4$ spin ground states for **5** and **6**, respectively.

Conclusions. The preparation of several tris(3,5-dimethylpyrazolyl)borate iron tricyanides and their use as building blocks to prepare magnetic clusters and networks have been described. Bridging tosylates also appear to be poor communicators of spin density information. Incorporation of isotropic manganese(II) centers into each structural archetype, while affording high-spin ground states, does not appear to contribute to the total anisotropy of derived compounds. Future efforts will investigate the treatment of cyanometalate squares with anisotropic ions, to attempt the preparation of one-dimensional chains of clusters.

Acknowledgment. S.M.H. gratefully acknowledges the donors of the American Chemical Society Petroleum Research Fund (Grant PRF 38388-G3), the Kentucky Science and Engineering Foundation (Grant KSEF-621-RDE−006), the University of Kentucky Summer Faculty Research

Fellow, and the University of Kentucky Major Research Project programs for financial support. G.T.Y. thanks the National Science Foundation (CHE-0210395) for financial support. S.M.H. is also grateful to Eugenio Coronado for providing the MAGPACK program. We are grateful to the reviewers for valuable suggestions.

Supporting Information Available: X-ray crystallographic data (CIF format, **2·H_2O-6**) and Supporting Information (additional magnetic data plots and crystallographic tables) are available in the Supporting Information. This material is available free of charge via the Internet at http://pubs.acs.org.

IC051044H